Fuel 88 (2009) 519–527

Contents lists available at ScienceDirect

Fuel

journal homepage: www.elsevier.com/locate/fuel

Gasification reaction kinetics on biomass char obtained as a by-product of gasification in an entrained-flow gasifier with steam and oxygen at 900–1000 °C

Keigo Matsumoto [a,*], Keiji Takeno [a], Toshimitsu Ichinose [a], Tomoko Ogi [b,1], Masakazu Nakanishi [b]

[a] Nagasaki Research and Development Center, Mitsubishi Heavy Industries, Ltd., 5-717-1 Fukahori-Machi, Nagasaki 851-0392, Japan
[b] Biomass Technology Research Center, National Institute of Advanced Industrial Science and Technology, 16-1 Onogawa, Tsukuba-shi, Ibaraki 305-8569, Japan

ARTICLE INFO

Article history:
Received 3 January 2008
Received in revised form 25 July 2008
Accepted 22 September 2008
Available online 20 October 2008

Keywords:
Biomass char
Gasification kinetics
Entrained-flow type gasifier

ABSTRACT

The purpose of this study was to investigate the gasification kinetics of biomass char, such as the wood portion of Japanese cedar char (JC), Japanese cedar bark char (JB), a mixture of hardwood char (MH) and Japanese lawngrass char (JL), each of which was obtained as a by-product of gasification in an entrained-flow type gasifier with steam and oxygen at 900–1000 °C. Biomass char was gasified in a drop tube furnace (DTF), in which gasification conditions such as temperature (T_g), gasifying agent (CO_2 or H_2O), and its partial pressure (P_g) were controlled over a wide range, with accompanying measurement of gasification properties such as gasification reaction ratio (X), gasification reaction rate (R_g), change of particle size and change of surface area. Surfaces were also observed with a scanning electric microscope (SEM). By analyzing various relationships, we concluded that the random pore model was the most suitable for the biomass char gasification reaction because of surface porosity, constant particle size and specific surface area profile, as well as the coincidence of R_g, as experimentally obtained from Arrhenius expression, and the value is calculated using the random pore model. The order of R_g was from 10^{-2} to 10^{-1} s^{-1}, when T_g = 1000 °C and P_g = 0.05 MPa, and was proportional to the power of P_g in the range of 0.2–0.22 regardless of gasifying agent. Reactivity order was MH > JC > (JB, JL) and was roughly dependent on the concentration of alkali metals in biomass feedstock ash and the O/C (the molar ratio of oxygen to carbon) in biomass char.

1. Introduction

As renewable sources of energy are being steadily introduced in many countries, for example, with the EU announcing that it intends to supply 20% of its overall energy needs from renewable sources by 2020, emphasis on biomass as a renewable source is growing. Accordingly, the development and establishment of advanced biomass utilization technologies are urgently required tasks. Among the more promising technologies, gasification and liquid fuel synthesis through gasification have the advantage of rapid conversion from large amounts and various kinds of biomass to easily storable and transportable gas or liquid fuel.

We developed a 240 kg/day-scale pilot plant under the auspices of a national project by the Ministry of Agriculture, Forestry and Fisheries of Japan [1]. Biomass was gasified in an entrained-flow type gasifier with steam and oxygen, the reactor of which was heated by an electric furnace, with methanol successfully synthesized from the product gas. The basic gasification properties of many kinds of biomass, including wood, grasses, agricultural residues and energy crops, were investigated to produce gas suitable for methanol synthesis. Based on pilot plant experiments and results, we developed a 2 ton/day-scale test plant, in order to verify system operations, to analyze gasification properties and to establish a gasification model for the design of a commercial scale plant in the context of a national project organized by the New Energy and Industrial Technology Development Organization (NEDO) [2]. This test plant was the first successful complete system for synthesizing methanol with a stand-alone entrained-flow gasifier, in which 2 ton of biomass per day were gasified with steam and oxygen to produce gas suitable for methanol synthesis and to generate heat so as to maintain a sufficiently high temperature for gasification without external heating. Although the cold gas efficiency and methanol synthesis yield of the test plant were quite high (>60% and >20 wt%, respectively), and the estimated performance of a commercial plant is considerably higher (the cold gas efficiency >75% and methanol synthesis yield >40 wt%), both would be improved of approximately 5% by gasifying char (char recycling), which is a by-product of gasification.

A number of studies have been performed on char produced from several kinds of biomass to coal, which were usually pyrolyzed in inert gas for a long enough period of time to ignore the

* Corresponding author. Tel.: +81 95 834 2400; fax: +81 95 834 2505.
E-mail addresses: keigo_matsumoto@mhi.co.jp (K. Matsumoto), t-ogi@aist.go.jp (T. Ogi).
[1] Tel.: +81 29 861 5567; fax: +81 29 861 8181.

0016-2361/$ - see front matter © 2008 Elsevier Ltd. All rights reserved.
doi:10.1016/j.fuel.2008.09.022

Nomenclature

A_0	ash content in char before gasification in the DTF (%)
A	ash content in char after gasification in the DTF (%)
A_a	pre-exponential factor (1/s)
C_0	carbon content in char before gasification in the DTF (%)
C	carbon content in char after gasification in the DTF (%)
d_p	median diameter (μm)
E_a	activation energy (kJ/mol)
F_c	carbon flow rate in supply char (g/h)
F'_c	carbon flow rate in char after gasification in the DTF (g/h)
F_g	carbon flow rate in gasifier gas (g/h)
K_r	reaction rate of the char when $X = 0$ (1/s)
L_0	initial micro pore length per unit solid volume (including voids) (m/m^3)
N	the exponent number of the partial pressure of the gasifying agent for the gasification reaction (–)
P_{CO_2}	partial pressure of CO_2 (MPa)
P_g	partial pressure of the gasifying agent (MPa)
P_{H_2O}	partial pressure of H_2O (MPa)
P_t	total pressure (MPa)
S	micro pore surface area per unit solid volume (including voids) (m^2/m^3)
S_0	initial micro pore surface area per unit solid volume (including voids) (m^2/m^3)
S_a	specific surface area (m^2/g)
t	reaction time in the DTF (s)
T_g	temperature of the DTF (°C)
X	reaction ratio of biomass char calculated from gas component in the DTF (–)
X_A	reaction ratio of biomass char calculated from char content in the DTF (–)
X_c	carbon conversion ratio of biomass in the test plant or pilot plant (–)
X_e	estimated reaction ratio of biomass char with Eq. (5) (–)
X_m	measured reaction ratio of biomass char calculated from the gas component in the DTF (–)
ε_0	initial void percentage (–)
ψ	structure parameter (–)

effect of their volatile materials, and several models have been based on these studies [3–6]. However, it was also reported that gasification properties of char were strongly dependent on the conditions of pyrolysis; the gasification reaction rate of rapidly pyrolyzed char with H_2O or CO_2 was three times faster than that of slow-pyrolyzed char [7], and char pyrolyzed at higher than 1200 °C was thermally deactivated [8–9]. Moreover, biomass was partially combusted in the entrained-flow gasifiers, and the possibility therefore had to be considered that the gasification kinetics of biomass char, gasified with O_2 and H_2O, were different from the previously reported results.

The purpose of this study was to investigate the gasification kinetics of char obtained from the 2 ton/day-scale test plant and from the 240 kg/day-scale pilot plant by using a drop tube furnace (DTF), and to formulate the reaction rates.

2. Methods

2.1. Biomass sample

Four kinds of biomass char were selected, consisting of the wood portion of Japanese cedar (JC), Japanese cedar bark (JB), a mixture of hardwood (MH), and Japanese lawngrass (JL). Japanese cedar is the most widely available woody biomass in Japan. MH is often mixed with waste wood or thinned wood. JL, which is also common in Japan, was selected as a representative grass. Only JL char was obtained from the aforementioned 240 kg/day-scale pilot plant, the temperature distribution of which was similar to the 2 ton/day-scale test plant.

The chemical analysis data for the test samples are shown in Table 1. The ash content of JC is the lowest of the four kinds of biomass. Although the elemental components of JB (C, H, O and ash) are similar to the wood type samples (JC and MH), its gasification properties are different due to high lignin content. The gasification properties of JB char were expected to be different from other biomass char. While potassium is known to accelerate the gasification reaction, many potassium salts vaporize at around 900–1000 °C, and the high potassium content of MH affects the gasification properties of MH and MH char. The rate of the gasification reaction is proportional to surface area, and the small surface area of JL char is attributable to its high SiO_2 content, just as with any kind of grass.

Each sample was classified between 50 and 100 μm (except for JL char, the maximum size of which was under 50 μm), and dried for 10 h at 50 °C.

2.2. Char analysis

Physical properties such as specific surface area, size distribution, and surface state of biomass char before and after gasification with DTF were analyzed. The specific surface area of biomass char was determined by physisorption of N_2, and the sorption isotherms were analyzed using the BET-method. The size distribution of biomass char was analyzed with a granulometer, and the surface state of biomass char was observed by means of an SEM.

2.3. Experimental apparatus

Fig. 1 shows a schematic view of the drop tube furnace (DTF) employed in the gasification tests. The pre-mixed gasifying agent (CO_2 or H_2O) and inert gas (N_2) were distributed to a pre-heater and char feeder, and then introduced into the reactor. The char feeder was a rotational knife-edge type, with char feeding into the reactor at a constant rate of 1–10 g/h. A ceramic cylinder with an inner diameter of 30 mm and a length of 500 mm was used as the reactor. Divided two-stage electric heaters surrounded the reactor in order to control the gas temperature within. The reaction time in the reactor was adjusted between 0.5 and 3 s by changing the height of the inlet through which biomass was delivered into the reactor and by changing the flow rate of the gasifying agent. The gasifying agent flowing through the reactor was heated with an electric heater to a predetermined value in the range of 900–1200 °C, while the pressure in the reactor was controlled by means of a pressure valve at the gas outlet. Total pressure (P_t) and the partial pressure of the gasifying agent (P_g) were set at 0.4 MPa and 0.025–0.3 MPa, respectively. Exhaust gas was analyzed with a gas chromatograph after water was removed with a gas cooler.

3. Results and discussion

No current model precisely expresses the gasification reaction of biomass char, since a spherical shape is assumed in every model, while the actual shape of char is different. However, the random

Table 1
Elemental and chemical analyses table for test samples (dry basis)

	Biomass feedstock							Ash content of biomass feedstock						Biomass char				X_c (%)
	C (wt%)	H (wt%)	O (wt%)	Ash (wt%)	Extract (wt%)	Lignin (wt%)	Holo (wt%)	SiO_2 (wt%)	Al_2O_3 (wt%)	Fe_2O_3 (wt%)	CaO (wt%)	K_2O (wt%)	Na_2O (wt%)	C (wt%)	H (wt%)	O (wt%)	Ash (wt%)	
JC	50.4	6.0	43.1	0.36	2.8	32.2	65.0	4.0	0.9	2.9	36.0	13.4	1.8	72.5	1.4	10.4	15.7	96.1[c]
JB	49.7	5.6	41.4	0.90	3.0	40.5	56.5	31.7	8.0	3.5	25.2	7.0	2.0	75.6	1.3	11.5	11.6	88.2[c]
MH	48.2	5.8	45.1	0.74	3.0	24.6	72.4	1.5	0.7	1.0	35.3	18.3	0.6	62.3	1.4	14.6	11.5	95.6[c]
JL[a]	47.1	6.1	37.9	6.38	3.5	18.4	78.1	75.1	4.9	2.2	5.9	3.7	0.4	13.0	0.3	1.6	85.1	97.9[d]
Coal[b]	–	–	–	–	–	–	–	–	–	–	–	–	–	81.7	0.7	2.4	14.1	–

[a] After pre-treatment.
[b] Referenced from [11].
[c] Gasified with 2 ton/day-scaled test plant.
[d] Gasified with 240 kg/day-scaled pilot plant.

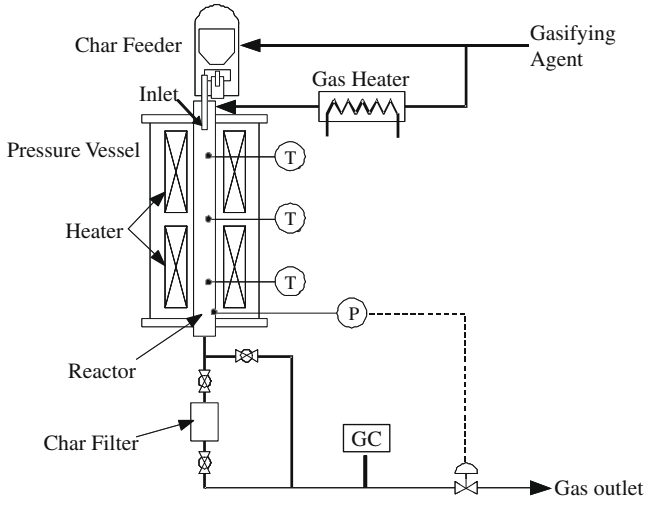

Fig. 1. Schematic flow of the drop tube furnace (DTF).

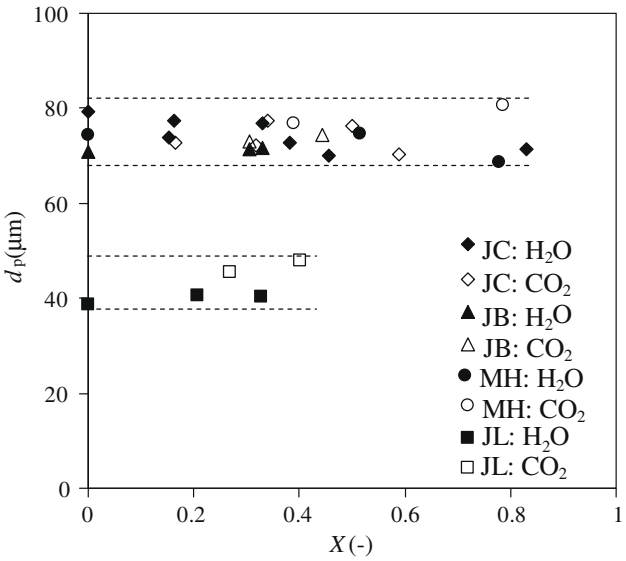

Fig. 2. Profile of median diameter of biomass char during gasification in DTF; dashed lines are the range of mean diameter measured with a granulometer.

pore model is the most suitable, as explained in Section 3, because measurable properties averaged over huge numbers of char particles of various shapes converge to those of spheres. We determined the parameters of the model from temperature to pressure dependences.

3.1. Model selection

Fig. 2 indicates the relationship between the median diameter (d_p) of biomass char and the gasification reaction ratio (X), which is defined as

$$X = \frac{F_g}{F_c} \tag{1}$$

where F_g and F_c represent the amount of carbon in exhaust gas and in the supplied char, respectively. The reaction models that include particle size change such as the shrinking core model [3] are not suitable for the present data, because the values of d_p depend only slightly on the value of X when $X < 0.8$. That is, the surface of the tested char is not uniform such that the gasification reaction initially occurs only at weak areas, and particle size (determined as the maximum outer dimension) is, thus nearly constant when $X < 0.8$. With respect to JC, JB and MH char, the effect of d_p on the gasification reaction can be ignored, since the d_p of these char types are in the range of 70–80 μm.

The accuracy of this experiment is mainly dependent on measuring X because measurement of particle size d_p is considerably more precise and reliable. Here, in order to estimate the accuracy of experimental data, X was also calculated from char collected in a char filter installed downstream from the reactor [10].

$$X_A = 1 - \frac{CA_0}{C_0A} \tag{2}$$

where C_0 and C represent the carbon concentration in char before and after gasification in the DTF, respectively. A_0 and A also represent the ash content in char before and after gasification in the DTF. Fig. 3 compares X_A and X. As a result, it was found that the experimental data were reliable because the difference between X and X_A was within about 10%.

Fig. 4 shows SEM images of JC char particles before and after gasification when X was about 0.8. It is observed that the d_p distributions of JC char are nearly constant before and after gasification regardless of the gasifying agent, although the sizes of the pores increase, which confirms the analyzed results of constant char particle size distribution in a granulometer (Fig. 2). Given the porous surface and constant particle size, we subsequently examined the

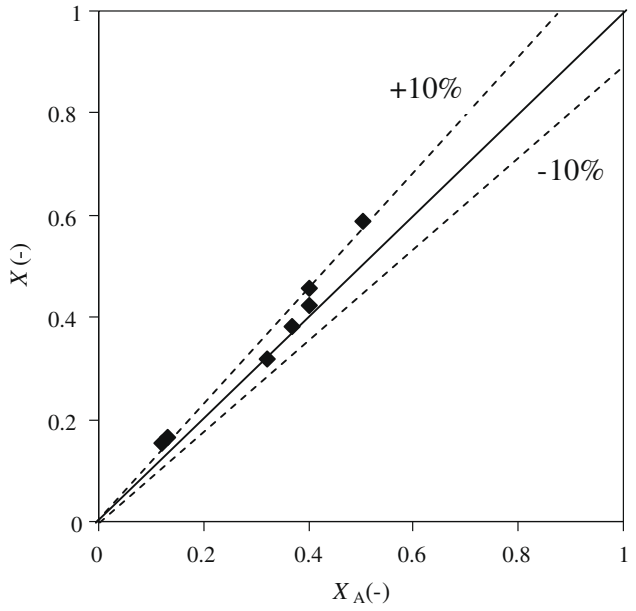

Fig. 3. Comparison of reaction ratio of JC char calculated from gas component (X) and that calculated from char content (X_A).

random pore model [11] and the grain model. Although micro pores, where the gasification reaction mainly occurs, are too small to be observed by SEM, the porous surface of char suggests the growth of micro pores inside. As no ash melting or degradation was observed, the surface of JC char is also about the same after gasification regardless of the gasifying agent. Hence, gasification kinetics of biomass char is well formulated by means of analyzing the profile of surface area of biomass char during gasification in the DTF. The surfaces of the other kinds of char are also porous as shown in Fig. 5. With respect to JL char only, the surface is rough and it is assumed to physically break down easily. Table 2 shows S_a for each char type before gasification measured using the BET-method. In particular, the S_a of JL char is much smaller than the others, as well as being characterized by a smaller d_p (Fig. 2). JL char was observed to physically break down prior to sufficient growth of the micro pores, due to the high SiO_2 content in the JL ash (Fig. 5) melting the micro pores and blocking growth.

The random pore model assumes that the reaction occurs on the inside surface of the micro pores, which occupy most of the surface area of the particles. According to the progress of the reaction, the surface area of the micro pores increase initially due to the growth of the diameter, and then decrease as the expanded pores overlap each other. The surface area of micro pores is described by the following equations

$$\frac{S}{S_0} = (1-X)\sqrt{1-\psi\ln(1-X)} \tag{3}$$

where

$$\psi = \frac{4\pi L_0(1-\epsilon_0)}{S_0^2} \tag{4}$$

The gasification reaction is assumed to occur at the micro pore surfaces, only where the gasification agent (H_2O or CO_2) exits. The gasification reaction rate (R_g) is proportional to S:

$$R_g = \frac{dX}{dt} = k_r(1-X)\sqrt{1-\psi\ln(1-X)} \tag{5}$$

where the gasification reaction rate (k_r), equal to the value of R_g when $X = 0$, was formulated as below [11]:

$$k_r = R_g|_{X=0} = P_g^n A_a \exp\left(-\frac{E_a}{RT_g}\right) \tag{6}$$

The structure parameter (ψ) of JC char was determined by fitting the obtained S/S_0 profile at each stage of gasification to the calculated value of the right side in Eq. (3) [12]. The relationship between X and the dimensionless surface area ratio (S/S_0) of JC char is shown in Fig. 6. The specific surface area (S_a) initially increases as the gasification reaction proceeds, then decreases. When $X = 0.3-0.4$, S_a reaches the maximum for both H_2O and CO_2. H_2O is observed to be more reactive than CO_2. The values of ψ are estimated to be approximately 10 for JC char.

When applying the grain model, the calculated dependence of R_g on X, which is subject to steady decrease, is not consistent with the experimental data (Fig. 6). The grain model was, therefore, deemed unsuitable.

Fig. 7 shows the measured time dependence of X for JC char, $X_m(t; T_g, P_g)$, at 900, 1000 and 1200 °C, and in H_2O or CO_2, the partial pressure of which was controlled to be approximately 0.2 MPa. $X_e(t; k_r)$ can be estimated by integrating Eq. (5) and by inserting $\psi = 10$ and $X_e(0; k_r) = 0$. Each line was drawn by adjusting k_r to minimize the sum of squares of the errors, $\sum(X_m - X_e)^2$. Each estimated dependence, $X_e(t; k_r)$, was well-fitted with the experimental values, $X_m(t; T_g, P_g)$, especially when $T_g = 1200$ °C, thus confirming that the random pore model was the most suitable and that the structure parameter of ten was the best estimate. The measured range of t was limited when $T_g = 900$ or 1000 °C because gas flow in the DTF became unstable when $t > 3$ s. Although measurement accuracy at 900 or 1000 °C was not especially high compared to that at 1200 °C, $R_g = dX/dt$ in H_2O was apparently lower than that in CO_2 when $T_g = 900$ °C, about the same when $T_g = 1000$ °C, and higher when $T_g = 1200$ °C. Temperature dependence is discussed in the Section 3.2.

3.2. Determining model parameters for formulation

In order to formulate the gasification reaction, X_m of four kinds of char were measured under various conditions and each $k_r = R_g(X = 0)$ was estimated.

3.2.1. Dependence of the gasification reaction rate on temperature

The dependence of $k_r = R_g(X = 0)$ on the temperature of the DTF (T_g) is represented in Fig. 8. Thick lines and thin lines indicate the linear fittings of JC when $P_g = 0.05$ and 0.2 MPa, respectively, and the dashed line references reported coal char data when $P_g = 0.25$ MPa [12]. The measured k_r for both H_2O and CO_2 gasifications were linearly dependent on $1/T_g$, which is known as the Arrhenius expression. It was confirmed that the random pore model was the most suitable among those examined for biomass char gasification.

From the linear fittings, activation energy (E_a) was estimated to be 136 or 93.9 kJ/mol for H_2O or CO_2 gasification, respectively. The estimated E_a of JC char was within the reported range corresponding to coal char (89–246 kJ/mol in H_2O and 96–297 kJ/mol in CO_2 at 950 °C, when $P_g = 0.03$ MPa, respectively), depending on fuel properties such as the pore structure of char, constituents of ash, char formation conditions and carbon structure [13]. In general, E_a of biomass char in the case of CO_2 gasification is larger than for H_2O gasification, especially when temperature is lower than 950 °C [13,14]. With regard to these experimental results, E_a of JC char for H_2O gasification was measured as being larger than in the case of CO_2 gasification. Takarada et al. also found the same tendency of reactivity for coal char having a low fuel ratio [13]. Moreover, similar results were obtained in other studies [15–16]. Ye et al. reported nearly the same value of E_a (131 kJ/mol for H_2O gasification and 91 kJ/mol for CO_2 gasification) with south Austra-

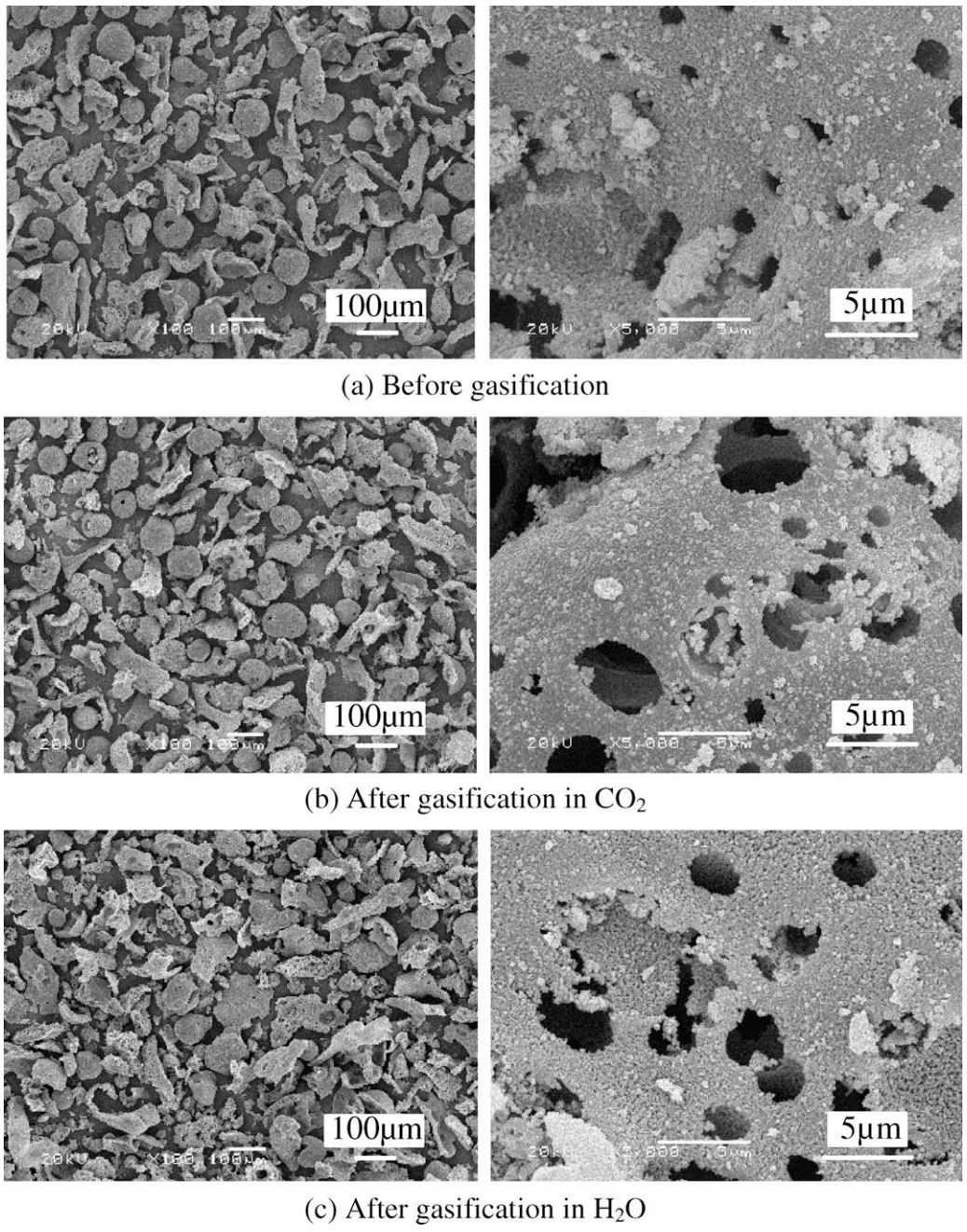

Fig. 4. Comparison of the surface state of JC char before and after gasification (X = approximately 0.8) in DTF; graphics are SEM images.

lian low-grade coal, and explained that the difference in rates for these two reactions is due to a greater number of active sites generated by H_2O than by CO_2 [15].

Accordingly, it was considered that E_a for H_2O gasification tends to be higher than CO_2 gasification under conditions of high gasification reaction rate such as at high temperature (more than 950 °C), with biomass or low-grade coal. It appears that multiple factors are involved, including the pore structure, the carbon structure, the number of active sites, and the obstruction of gasification by generated H_2 or CO in the micro pores due to the high gasification reaction rate. Furthermore, the tested char was generated at a high concentration of H_2O, unlike the cases generally reported. It is also possible that this difference in char formation conditions affects the value of E_a. However, the mechanism of the difference of E_a between the gasifying agents has not yet been clarified, owing to its complexity.

The order of R_g, when $X = 0$, was between 10^{-2} and 10^{-1} s^{-1} for both H_2O and CO_2 gasifications, at P_g = 0.05–0.2 MPa and T_g = 900–1000 °C, and was five times larger than that of coal char made by means of de-volatilization of sub-bituminous coal with a low fuel ratio (1.07). This high reactivity is inherent in biomass char and not attributable to the difference in the char-making processes, because the value of R_g obtained for the tested biomass char is the same order as that of rapidly pyrolyzed char in inert gas. Zhang et al. reported a gasification reaction rate of 10^{-2}–10^{-1} s^{-1} on coffee grounds and JB char, rapidly pyrolyzed in advance at 1200 °C in a DTF, when $X = 0$, $P_{CO_2} = 0.2$ MPa and T_g = 1000 °C [17]. The R_g of the tested char was assumed to be greater than for pyrolyzed char,

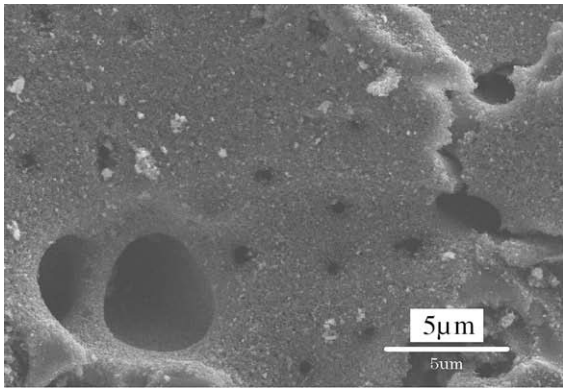

(a) JB

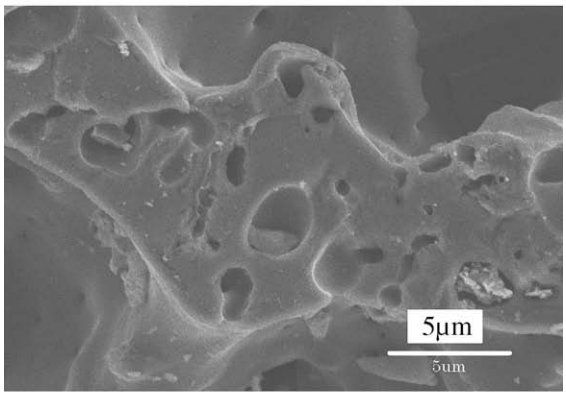

(b) MH

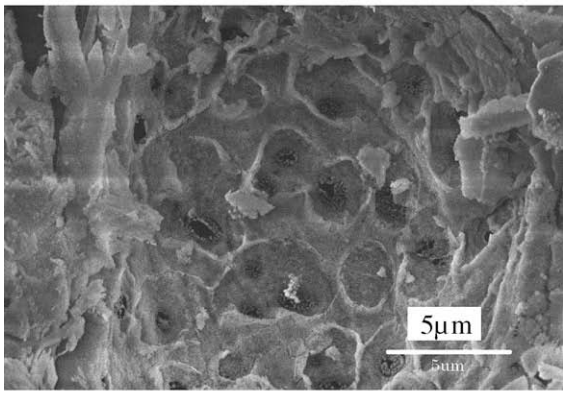

(c) JL

Fig. 5. Comparison of the surface state of JB, MH, and JL char before gasification in DTF; graphics are SEM images.

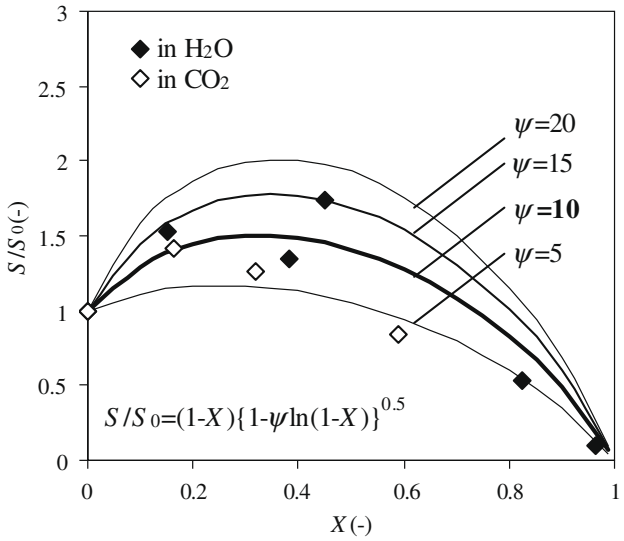

Fig. 6. Profile of JC char dimensionless surface area during gasification in DTF; plots are the experimental data, and lines are calculated values using the random pore model.

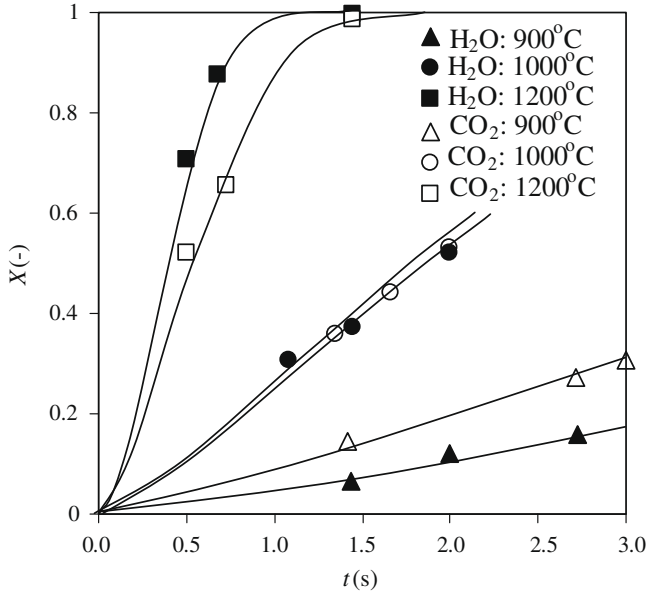

Fig. 7. Gasification reaction ratio (X) of JC char during H_2O or CO_2 gasification when P_g = 0.2 MPa with DTF; lines were drawn by estimating $X(t; k_r)$ through integration of Eq. (5) and insertion of ψ = 10 and $X(0; k_r) = 0$.

Table 2
Specific surface area of biomass char (dry basis)

	S_a (m^2/g)
JC	184
JB	379
MH	204
JL	40

since pyrolysis and the gasification reaction occurred faster when O_2 and H_2O exists.

On the other hand, the value of R_g obtained for each char type is greater than the reported gasification reaction rate values for biomass char [14,18]. It was considered that the difference of R_g between the tested char and reported values is due to the difference in char-making conditions. Generally, char was made at relatively low temperatures (approximately 800–900 °C), with a low heating rate for sufficient time in inert gas in order to ignore the effect of volatile matter. The quick de-volatilization of the fuel in rapid pyrolysis favors the formation of char with high porosity and high reactivity [19].

3.2.2. Dependence of the gasification reaction on the partial pressure of gasifying agents

Fig. 9 shows the dependence of $k_r = R_g(X = 0)$ on P_g. Solid lines connect the experimental data of each char type under the same conditions except P_g.

R_g of JC char is proportional to the 0.22 power of P_g at 900–1200 °C regardless of the gasifying agent. Accordingly, the pre-exponential factors (A_a) of JC char were estimated to be

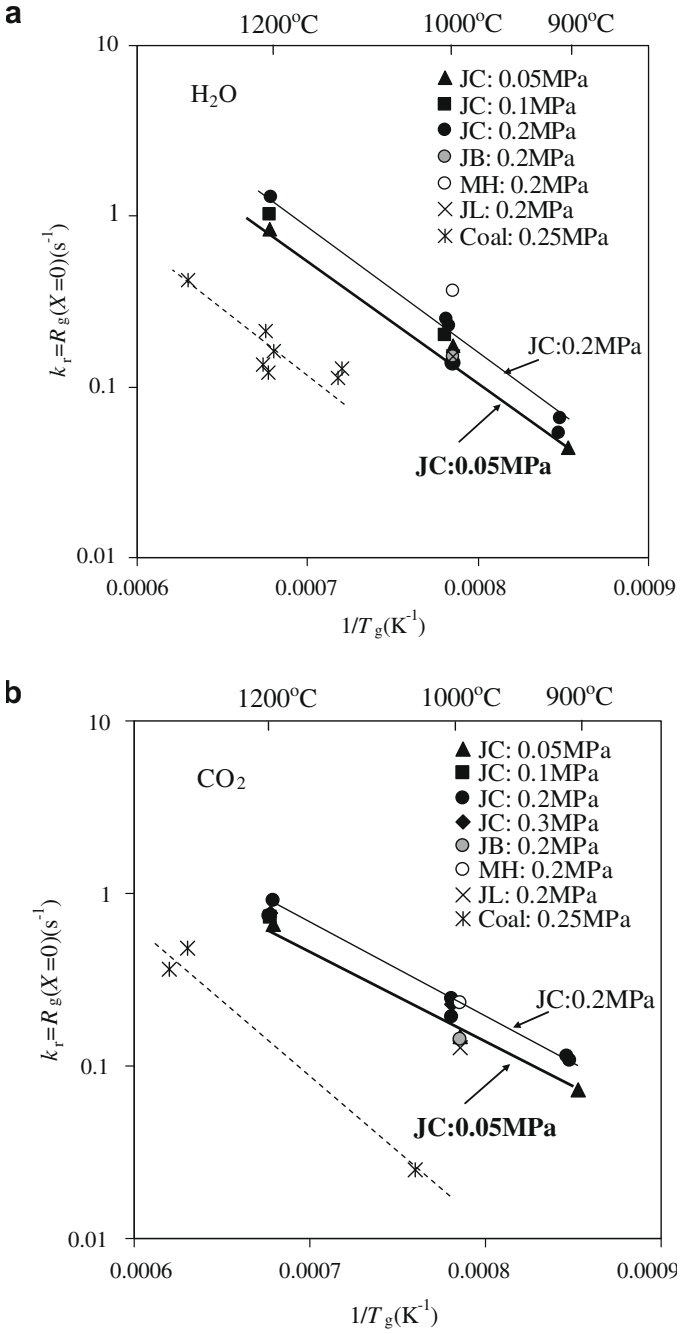

Fig. 8. Dependence of the gasification reaction rate of char (R_g) according to the random pore model on the temperature ($X = 0$, above: in H_2O gasification, below: in CO_2 gasification); thick lines and thin lines were drawn by connecting the experimental data for JC when $P_g = 0.05$ and 0.2 MPa, respectively, with the dashed line referencing reported coal char data when $P_g = 0.25$ MPa [11].

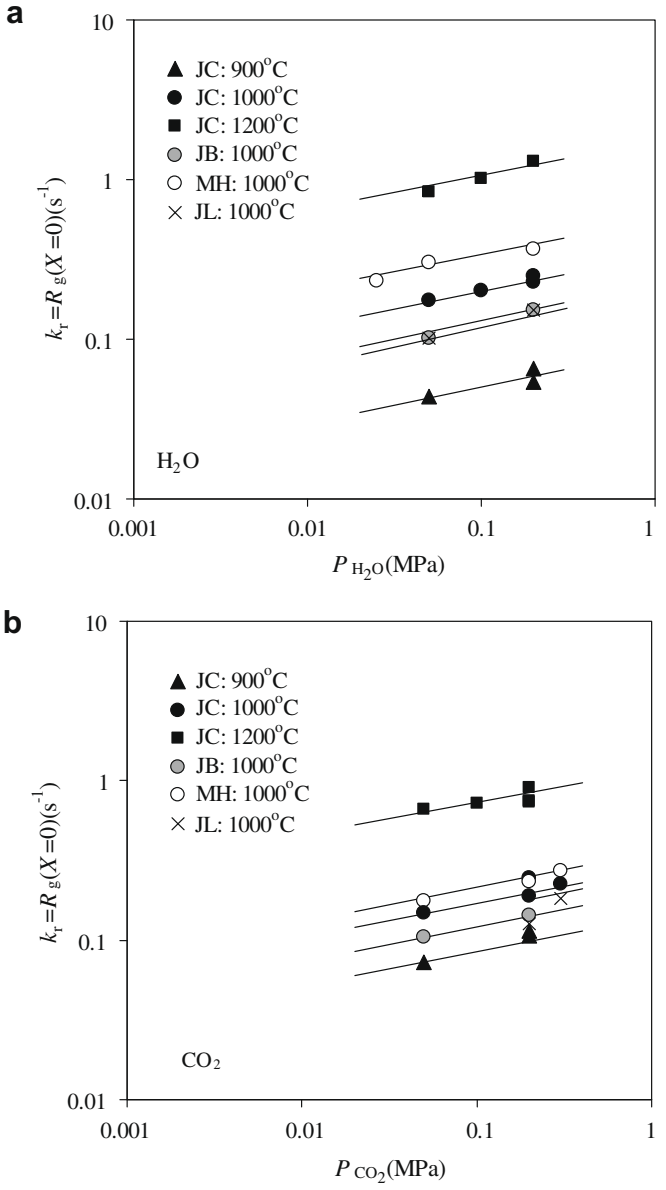

Fig. 9. Dependence of the gasification reaction rate of char (R_g) according to the random pore model on the gasifying agent partial pressure (P_g) ($X = 0$, above: in H_2O gasification, below: in CO_2 gasification); solid lines were drawn by connecting the experimental data for each type of char.

9.99×10^4 and 2.24×10^3 s^{-1} $MPa^{-0.22}$ for H_2O and CO_2 gasifications, respectively.

Based on the above results, the gasification reaction rate (R_g) of JC char was estimated as below

$$H_2O\,\text{gasification}: R_g = P^{0.22}\,9.99 \times 10^4 \exp\left(-\frac{136}{RT}\right) (1-X)\sqrt{1-10\ln(1-X)}$$

$$CO_2\,\text{gasification}: R_g = P^{0.22}\,2.24 \times 10^3 \exp\left(-\frac{93.9}{RT}\right) (1-X)\sqrt{1-10\ln(1-X)}$$

The values of n of the other kinds of char are also in the range of 0.2–0.22. These exponent numbers are smaller than previously reported values. For example, the exponent numbers of grapefruit char and coal char, pyrolyzed over 1–2 h at 700–1000 °C, are reported to be 0.5–0.6 and 0.32–1.1, respectively [13,20].

These results indicate that biomass char, which is gasified with at least 4 s in steam and oxygen at 900–1000 °C, has a high reactivity even at low P_{CO_2} or P_{H_2O}, probably because oxygen and hydrogen remain in the char. With regard to hydrogen, Rassel et al. reported that hydrogen remaining in the char after pyrolysis at 1000 °C contributed to high reactivity of the char [21,22]. The oxygen in organic carbons or chemical compounds, given by subtracting carbon, hydrogen, nitrogen, sulfur and ash from 100%, still amounted to 10–20%, regardless of the kinds of biomass, because oxygen with metal (metal oxide) was counted as ash in the analysis, although the percentage of carbon and hydrogen in biomass char decreased with gasification progress as shown in Fig. 10. However, the exis-

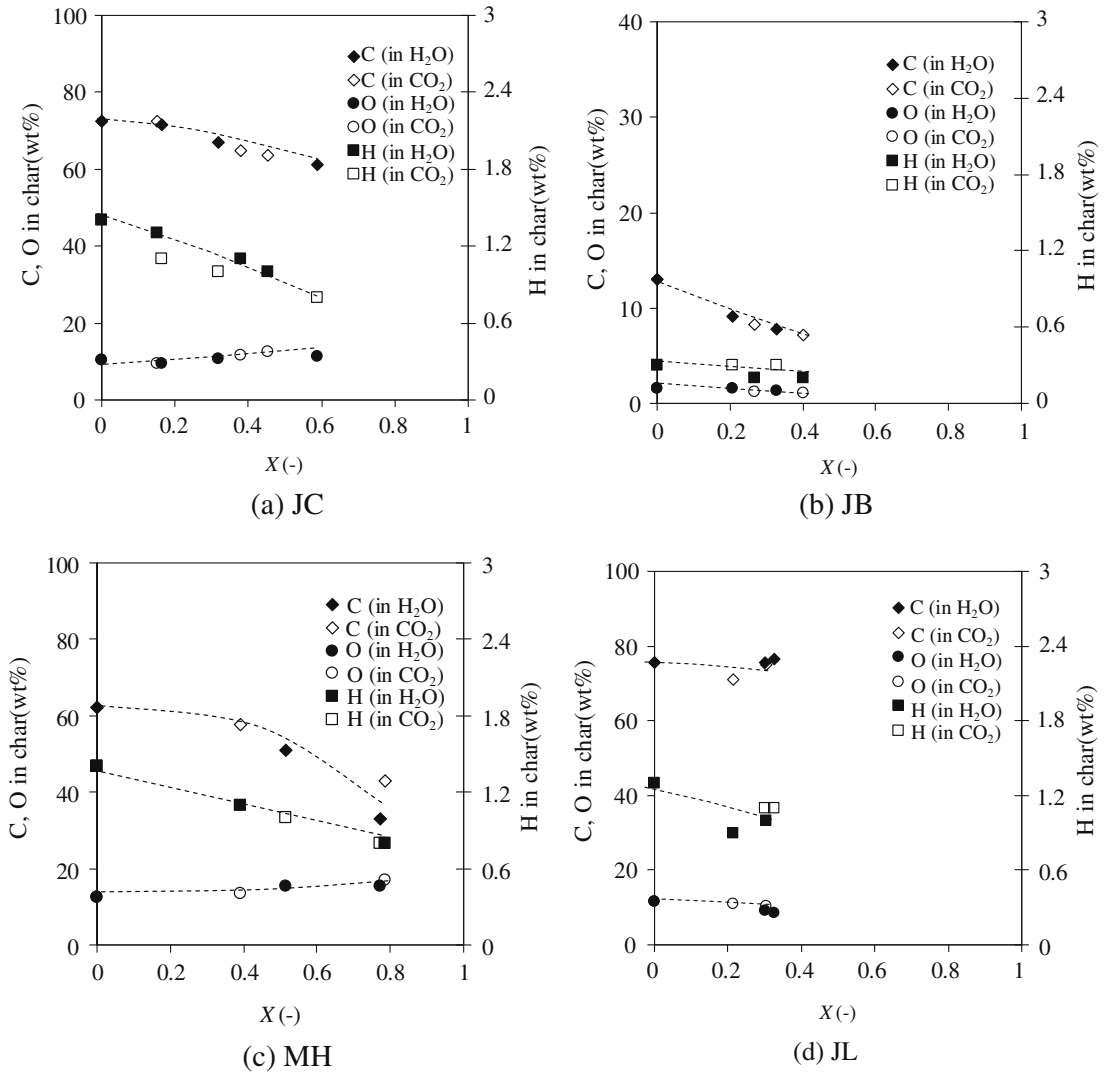

Fig. 10. Profile of C, H and O concentration in char during gasification; dashed lines were drawn by connecting averaged experimental data.

tence of oxygen and its reaction kinetics in char are issues for future study.

3.3. Comparison of the reaction rates of each type of char

The CO_2 or H_2O reactivity order of the tested char is MH > JC > (JB, JL) as indicated in Fig. 9. The concentration of ($K_2O + Na_2O$) in biomass feedstock ash is related to the value of R_g for biomass char as shown in Fig. 11. This result is of practical interest for the utilization of unknown biomass as gasification feedstock, because R_g is estimable from ($K_2O + Na_2O$) content. The catalytic effect of alkali metals on progressing gasification reactions is well known [23], and Feng et al. reported the effects of inorganic additives such as alkali metals to cellulose [24]. It is generally assumed that the catalytic effect takes place in a catalytic redox cycle, in which the oxygen is transferred to the carbon surface from the metallic catalyst present in this surface [25]. The effect of ($K_2O + Na_2O$) for H_2O gasification is observed to be stronger than for CO_2 gasification, and there is a possibility that other factors are related.

Additionally, oxygen in char is considered to increase the char reactivity, because O/C (the molar ratio of oxygen to carbon) of char is also roughly dependent on R_g (Fig. 12). Takarada et al. also concludes that O/C related with R_g on coal char [13]. O/C is also

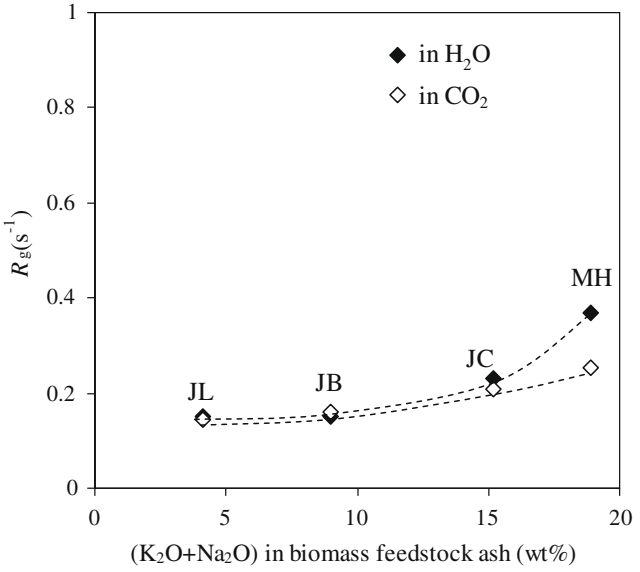

Fig. 11. Relationship between the concentration of alkali metals in the ash of biomass feedstock and the gasification reaction rate of char (R_g) (X = 0, 1000 °C, and P_g = 0.2 MPa); dashed lines were drawn by connecting the experimental data for each type of char.

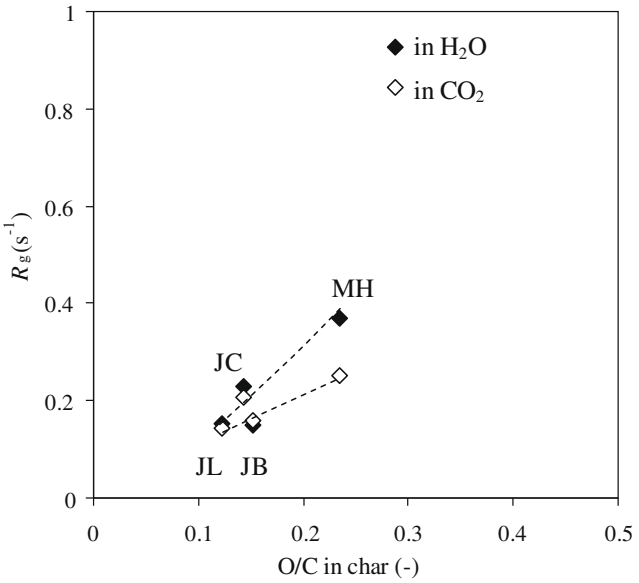

Fig. 12. Relationship between the O/C of char and the gasification reaction rate of char (R_g) (X = 0, 1000 °C, and P_g = 0.2 MPa); dashed lines were drawn by connecting the experimental data for each type of char.

useful for estimating the R_g of unknown biomass, although it is subject to char-making conditions. On the other hand, other char properties such as the carbon conversion ratio from biomass feedstock in the 240 kg/day-scale pilot plant or 2 ton/day-scale test plant (X_c), H/C or S_a of biomass char are unrelated to R_g (Tables 1 and 2).

4. Conclusions

We investigated the gasification kinetics of four kinds of biomass char obtained from an entrained-flow type gasifier with steam and oxygen at 900–1000 °C, using a drop tube furnace. The tested char had high reactivity, which was five times greater than that of coal char formed through de-volatilization of sub-bituminous coal with a low fuel ratio (1.07). This higher reactivity also remained at a relatively low partial pressure of gasifying agent (P_g = 0.5 MPa). It is considered that not only the original high reactivity of biomass char but also rapid pyrolysis and oxygen remaining in char are related.

By applying these data to the random pore model, based on considerations involving surface porosity, constant particle size, specific surface area profile, we formulated the gasification reaction rate (R_g) of Japanese cedar (JC) char in H_2O or CO_2. These equations are useful for many applications, such as designing a char recycling system or an entrained-flow type gasifier itself. Additionally, we found that the CO_2 and H_2O reactivity order was MH > JC > (JB, JL) and was related to the concentration of alkali metals and the O/C in biomass char. Accordingly, when other kind of char are used, the R_g of biomass char can be estimated in advance from the concentration of alkali metals in biomass feedstock and the O/C of biomass char.

Acknowledgement

The authors would like to express their sincere thanks to NEDO (the New Energy and Industrial Technology Development Organization), who organized and fiscally supported this research.

References

[1] Nakagawa H, Harada T, Ichinose T, Takeno K, Matsumoto S, Kobayashi M, et al. Biomethanol production and CO_2 emission reduction from forage grasses, trees and residues of crops. In: Proceedings of the third symposium on greenhouse gases and carbon sequestration in agriculture and forestry, 2005.
[2] Matsumoto K, Takeno K, Ichinose T, Ishii H, Nishimura K. Development of a 2 ton/day-scale test plant for total operation study of woody biomass gasification and liquid fuel synthesis. In: Proceedings of the fifteenth European biomass conference and exhibition, 2007. p. 1945–50.
[3] Bhat A, Bheemarasetti JVR, Rao TR. Kinetics of rice hask char gasification. Energ Convers Manage 2001;42:2061–9.
[4] Kajitani S, Hara S, Matsuda H. Gasification rate analysis of coal char with a pressurized drop tube furnace. Fuel 2002;81:539–46.
[5] Colomba DB, Federico B, Carmen B. Reactivities of some biomass char in air. Carbon 1999;37:1227–38.
[6] Truls L, Krister S. Modelling of char–gas reaction kinetics. Fuel 1997;76: 29–37.
[7] Chen G, Yu Q, Sjoestroem K. Reactivity of char from pyrolysis of birch wood. J Anal Appl Pyrolysis 1997;40(41):491–9.
[8] Shim HS, Hurt RH. Thermal annealing of chars from diverse organic precursors under combustion-like conditions. Energ Fuel 2000;14:340–8.
[9] Zolen A, Jensen AD, Jensen PA, Dam J. Experimental study of char thermal deactivation. Fuel 2002;81:1065–75.
[10] Bhatia SK, Perlmutter DD. A random pore model for fluid–solid reactions: I. Isothermal, kinetic control. AIChE J 1980;26:379.
[11] Ahn DH, Gibbs BM, Ko KH, Km JJ. Gasification kinetics of an Indonesian sub-bituminous coal char with CO_2 at elevated pressure. Fuel 2001;80:1651–8.
[12] Takashima R, Yokohama K, Takeno K, Akimoto A. Construction of a char gasification reaction model at high temperature and high H_2O partial pressure. In: Proceedings of the ICCS&T, 2005.
[13] Takarada T, Ida N, Hioki A, Kanbara S, Yamamoto M, Kunii K. Estimation of gasification rate of coal chars in steam-nitrogen atmosphere. Nenryo-kyokaishi 1988;67:1061–9.
[14] Klose W, Woelki M. On the intrinsic reaction rate of biomass char gasification with carbon dioxide and steam. Fuel 2005;84:885–92.
[15] Ye DP, Agnew JB, Zhang DK. Gasification of a south Australian low-rank coal with carbon dioxide and steam: kinetics and reactivity studies. Fuel 1998;77:1209–19.
[16] Johnson JL. Fundamentals of coal gasification, chemistry of coal utilization. New York: Wiley Interscience; 1981.
[17] Zhang Y, Ashizawa M, Kajitani S, Miura K. Proposal of a semi-empirical kinetic model to reconcile with gasification reactivity profiles of biomass chars. Fuel 2008;87:475–81.
[18] Cetin E, Gupta R, Moghtaderi B. Effect of pyrolysis pressure and heating rate on radiata pine char structure and apparent gasification reactivity. Fuel 2005;84:1328–34.
[19] Zanzi R, Sjoestroem K, Bjoernbom E. Rapid high temperature pyrolysis of biomass in a free-fall reactor. Fuel 1996;75:545–50.
[20] Marquez MF, Cordero T, Rodriguez MJ, Rodriguez JJ. CO_2 and steam gasification of a grapefruit skin char. Fuel 2002;81:423–9.
[21] Russell NV, Gibbins JR, Man CK, Williamson J. Coal char thermal deactivation under pulverized fuel combustion conditions. Energ Fuel 2000;14:883–8.
[22] Russell NV, Gibbins JR, Williamson J. Structural ordering in high temperature coal chars and the effect on reactivity. Fuel 1999;78:803–7.
[23] Devi TG, Kannan MP. Gasification of biomass chars in air – effect of heat treatment temperature. Energ Fuels 2000;14:340–8.
[24] Feng J-W, Zhang S, Maciel GE. EPR investigations of the effect of inorganic additives on the charring and char/air interactions of cellulose. Energ Fuels 2004;18:1049–65.
[25] Encinar JM, Gonzalez JF, Rodriguez JJ, Ramiro MJ. Catalysed and uncatalysed steam gasification of eucalyptus char. Influence of variables and kinetic study. Fuel 2001;80:2025–36.